

Arousal defines the conditions for facilitation by L-DOPA of extinction consolidation and associated prefrontal activity

Andres, E.^{1+*}, Chuan-Peng, H.¹⁺, Gerlicher, A.M.V.^{2,3,4}, Meyer, B.^{1,2}, Tüscher, O.^{1,5}, Kalisch, R.^{1,2}

¹Leibniz Institute for Resilience Research (LIR), 55122 Mainz, Germany

²Neuroimaging Center (NIC), Focus Program Translational Neuroscience (FTN), Johannes Gutenberg University Medical Center Mainz, 55131 Mainz, Germany

³Department of Experimental Psychology, Helmholtz Institute, Utrecht University, 3584 CS Utrecht, The Netherlands

⁴Department of Clinical Psychology, University of Amsterdam, 1018 WS Amsterdam, The Netherlands

⁵Department of Psychiatry and Psychotherapy, Johannes Gutenberg University Medical Center, 55131 Mainz, Germany

⁺equal contribution

^{*}corresponding author (elena.andres@lir-mainz.de)

Abstract

Even after successful extinction, conditioned fear can return. Strengthening the consolidation of the fear-inhibitory safety memory formed during extinction is one way to counteract return of fear. In this preregistered direct replication study, we confirm that spontaneous post-extinction reactivations of a neural activation pattern evoked in the ventromedial prefrontal cortex (vmPFC) during extinction predict extinction memory retrieval 24 h later. We do not confirm that L-DOPA administration after extinction enhances retrieval and that this is mediated by enhancement of the number of vmPFC reactivations. However, additional preregistered analyses reveal a beneficial effect of L-DOPA on extinction retrieval when controlling for salivary alpha-amylase (sAA) levels, an indicator of arousal, at extinction onset. Further, pre-extinction sAA negatively predicts retrieval and (at trend) vmPFC reactivations, and these impeding effects are abolished by L-DOPA treatment. Our results suggest that L-DOPA may enhance extinction consolidation under high-arousal conditions, as typically present during exposure therapy sessions.

Introduction

Recognizing an event or situation as dangerous and reacting defensively when it re-occurs is a learning mechanism (fear or threat conditioning) that is fundamental for survival. However, learning when a previous threat no longer signals danger and ceasing costly defense behavior (fear or threat extinction) also has great adaptive value and has been related to a reduced risk for threat-related mental disorders such as post-traumatic stress disorder (PTSD) or anxiety disorders¹. Also, extinction learning is the probable mechanism that underlies the exposure-based treatment of threat-related disorders^{2,3}.

To investigate whether fear extinction lastingly reduces CRs, a three-phase paradigm is commonly used, consisting of fear conditioning, fear extinction, and a memory test. During fear conditioning, an innocuous conditioned stimulus (CS) is repeatedly paired with an unconditioned stimulus (US). Participants start to exhibit CRs to the formerly neutral CS, and a CS-US association, or ‘fear memory’, is formed⁴. During extinction, participants are re-exposed to the CS in the absence of the US several times, and CRs decrease. During the test phase, participants are once more exposed to the CS, again in the absence of the US, and CRs are measured. Based on this paradigm, studies have reported that even after a complete reduction of CRs over the course of extinction, CRs often return during the test phase (“return of fear”⁵). Thus, extinction learning is not an unlearning or erasure of the original fear memory, but formation of a new CS-noUS association or ‘extinction memory’⁵, and the test phase effectively examines the retrieval and/or expression of the fear in competition with the extinction memory.

In exposure-based treatment, relapse after successful exposure is not uncommon, and return of fear is presumably a precursor for relapse³. Therefore, it would be highly desirable to develop methods to prevent the return of fear. Given that consolidation processes are crucial for long-term memory expression⁶⁻⁸, reinforcing the consolidation of the extinction memory may be one promising avenue⁹.

The dopaminergic system plays a crucial role in memory consolidation¹⁰. In the case of extinction, memory retrieval has been shown to be worse when dopaminergic activity is decreased after extinction training. After microinfusion of a D1 receptor antagonist into the infra-limbic part of the medial prefrontal cortex (IL) following extinction training in rats, later extinction memory retrieval was reduced relatively to a vehicle condition, suggesting impaired consolidation¹¹. Conversely, increasing dopaminergic activity after extinction training results in better long-term extinction memory retrieval. So, the systemic administration in mice of methylphenidate, a dopamine and noradrenaline reuptake inhibitor, after extinction learning led to relatively decreased fear responses at test 24 h later¹². Of particular relevance for potential clinical applications, post-extinction systemic administration of the anti-Parkinson drug L-DOPA, a precursor of dopamine that preferentially enhances dopaminergic turnover in the frontal cortex¹³, improved extinction memory retrieval both in mice and healthy normal humans in altogether six experiments^{14–16}. A negative result in one human study was accompanied by reduced neural activity at test in brain areas related to conditioned fear¹⁷. In two human experiments conducted outside the magnetic resonance imaging (MRI) environment¹⁸, post-extinction L-DOPA reduced CRs at test only in participants who showed successful extinction learning; in one other non-MRI study, the L-DOPA effect was absent¹⁹. Hence, L-DOPA is a likely pro-consolidation agent, although the boundary conditions for its effectiveness still have to be established.

A strong body of research supports a causal role for the IL, the rodent homolog of the vmPFC, in the consolidation of extinction memories²⁰. In humans using functional MRI (fMRI), Gerlicher et al. (2018)¹⁶ reported that a neural activation pattern in the vmPFC, which they initially observed during extinction when the US was unexpectedly omitted from CS presentations, spontaneously re-occurred during post-extinction rest. They further observed that the number of reactivations of this multi-voxel pattern (MVP) in the resting state predicted extinction memory retrieval as well as vmPFC activation at the memory test 24 h later. Importantly, the IL/vmPFC is a target of dopaminergic projections from the ventral tegmental area (VTA), and

extinction has been shown to evoke lasting dopamine release in this brain area²¹. Extending the rodent microinfusion data¹¹, Gerlicher et al. (2018)¹⁶ also reported that post-extinction L-DOPA administration enhanced the number of spontaneous vmPFC MVP reactivations and that this mediated the beneficial effect of L-DOPA on extinction retrieval. No other brain area showed this relationship, suggesting a pro-consolidation action of dopamine that depends on consolidation-related vmPFC activity.

A further intriguing aspect of this study was that all findings were specific to vmPFC MVPs from early extinction trials. Early in extinction, the CS still elicits a high US expectation, and the surprise (or “prediction error”, PE) generated by US omission is highest²². It is generally accepted that the formation of the new CS-noUS association in extinction is driven by this PE²³⁻²⁵, and extinction PEs in turn have been shown to be encoded by phasic dopamine release in the ventral striatum²⁶. It is currently unclear whether the vmPFC also receives dopaminergic extinction PE signals, but extinction PE-correlated fMRI activity has been observed in humans also outside the ventral striatum²⁷. Taken together, the VTA-originating dopaminergic system may tie together extinction learning, memory formation, and memory consolidation via influences on the prefrontal cortex.

We here aimed to directly replicate the findings of Gerlicher et al. (2018)¹⁶, as preregistered in Chuan-Peng et al. (2018)²⁸. For this, we employed the same fMRI paradigm (Fig. 1a) with differential fear conditioning in context A (background picture) on day 1. Two geometric symbols served as CS+ (reinforced at its offset in 50% of conditioning trials with a painful US) and CS- (non-reinforced CS), respectively. Extinction learning in context B on day 2 was immediately followed by oral placebo or L-DOPA administration (randomized between-subject design) and resting-state fMRI scans 10, 45, and 90 min after the end of extinction, to cover the early consolidation window. On day 3, we tested extinction memory retrieval in context B. During extinction and test, no US was administered. Skin conductance responses (SCRs) were used as CRs (Fig. 1b).

We tested three main replication hypotheses²⁸: First, we expected that post-extinction L-DOPA as compared to placebo administration would improve extinction memory retrieval at test on day 3. That is, we expected smaller differential (CS+>CS-) SCRs for L-DOPA- compared to placebo-treated participants (hypothesis 1). Second, we expected that the number of spontaneous post-extinction reactivations during the post-extinction resting-state scans of a vmPFC MVP linked with CS+ offsets in the first five extinction trials (first third of extinction) would predict extinction memory retrieval during test on day 3 in both placebo- and L-DOPA-treated participants (hypothesis 2). We were particularly interested in the resting-state scan conducted 45 min after extinction, as this is where Gerlicher et al. (2018)¹⁶ had observed a predictive relationship to retrieval, but also allowed ourselves to test the scans conducted 10 and 90 min after extinction, as a precise timing of, or very restricted time window for, the effect was considered unlikely. Third, we expected that L-DOPA would significantly increase the number of vmPFC reactivations (hypothesis 3).

To determine the optimal replication sample size, we combined different approaches²⁸. We conducted a power analysis based on the critical effect size from Gerlicher et al. (2018)¹⁶ for the most important hypothesis 1 (see Methods for details). This led to a required sample size of N=22 (i.e., eleven participants per treatment group). However, considering that effects in discovery samples may overestimate the true effect size, Simonsohn (2015)²⁹ suggested that replication studies should have a sample size that is at least 2.5 times greater than that of the discovery study (N=40 in Gerlicher et al., 2018¹⁶), leading to a required sample size of N=100 (50 per group). This approach would mean that we would need a sample size 4.5 times bigger than the sample size estimated based on the critical effect size in the discovery study, which we considered exaggerated. To balance the feasibility of a three-day pharmacological fMRI paradigm and the requirement to limit the number of participants exposed to study-associated burden³⁰ with the requirement of sufficient statistical power, we settled on a sample size of N=70 (35 per group). With an estimated drop-out rate of 10%, this means we could expect to achieve a final sample size of N=63, which is 1.5 times greater than in the discovery study

and nearly 3 times greater than based on power calculation. The responsible medical ethics committee approved this approach.

We furthermore extended the paradigm to clarify two remaining questions (see preregistration²⁸). First, to assess whether L-DOPA not only protects against the spontaneous recovery of extinguished fear after a mere passage of time but also against the renewal of fear gated by a context change⁵, we added a test in a new context C (non-extinction context, a new background picture) on day 3 (secondary research question 1; Fig. 1a). Protection against renewal would suggest that L-DOPA makes the extinction memory context independent, as indicated by the results of Haaker et al. (2013)¹⁴. Second, we collected saliva samples throughout all experimental days to measure salivary alpha-amylase (sAA) and salivary cortisol (sCORT) levels as markers of the activity of the (nor)adrenergic system and of the hypothalamus-pituitary-adrenal gland (HPA) axis, respectively^{31,32} (Fig. 1c). Arousal and stress have been suggested to affect consolidation processes in general and extinction consolidation in particular^{33–35}. We had previously observed L-DOPA main effects in two out of three MRI experiments^{14,16,17}, while two purely behavioral experiments showed only conditional L-DOPA effects, moderated by prior extinction success¹⁸, and one other behavioral study showed no effect¹⁹. This might indicate a potential influence of the MRI environment on the effect of L-DOPA¹⁹. Previous studies have reported relatively increased sAA^{36,37} and sCORT levels^{36,38} in the scanner environment. It is conceivable that higher arousal or stress might impair extinction^{33,39}, leaving more room for an augmenting effect of L-DOPA; alternatively, dopamine might positively interact with arousal- or stress-related neural activity in its effect on extinction consolidation^{13,33}. We therefore wondered if peak sAA or sCORT levels on the extinction day 2 would affect extinction retrieval on day 3 and interact with treatment (placebo vs. L-DOPA) (secondary research question 2).

Results

Effect of L-DOPA administration post extinction on extinction memory retrieval

First, we tested whether post-extinction L-DOPA compared to placebo administration on day 2 enhances extinction memory retrieval on day 3 (preregistered hypothesis 1). We compared the extent of spontaneous recovery of CRs in the extinction context B between the two treatment groups (see Fig. 1b). In addition, we asked whether L-DOPA administration also reduces contextual renewal of fear in a new context C on the test day (preregistered secondary research question 1).

Fear acquisition on day 1 was equally successful in both groups, as indicated by a significant effect of stimulus (CS+>CS- SCRs averaged across last 20% trials: $F_{1,64}=70.52$, $p<.001$, generalized $\eta^2=.23$) in the absence of group (placebo/L-DOPA) and stimulus by group effects ($p>.33$, $n=66$ participants with sufficient SCR data quality; Fig. 1b; see Methods and Supplementary Table 2 for details on exclusions and resulting final sample sizes per analysis). Fear was retrieved at the beginning of extinction on day 2 in both groups (start-fear: averaged CRs across first 20% trials; stimulus: $F_{1,49}=36.23$, $p<.001$, generalized $\eta^2=.16$; group and stimulus*group: $p>.14$; $n=51$). By the end of extinction on day 2 (end-fear: SCRs across last 20% trials), an unforeseen group difference emerged (stimulus: $F_{1,49}=8.81$, $p=.005$, generalized $\eta^2=.04$; group: $F_{1,49}=2.07$, $p=.16$; stimulus*group: $F_{1,49}=4.92$, $p=.02$, generalized $\eta^2=.02$, $n=51$), characterized by higher CRs towards the CS+ in the placebo group (two-sample t-test: $t_{49}=2.09$, $p=.04$, CI 95% [0.006 0.31]).

Contrary to our predictions, administration of L-DOPA on day 2 did not result in a significant reduction of spontaneous recovery on day 3 (averaged CRs across all trials; stimulus: $F_{1,53}=55.30$, $p<.001$, generalized $\eta^2=.20$; group: $F_{1,53}=.91$, $p=.34$; stimulus*group: $F_{1,53}=0.02$, $p=.89$; $n=55$). Also, contextual renewal of fear was not reduced (stimulus: $F_{1,53}=23.66$, $p<.001$, generalized $\eta^2=.07$; group: $F_{1,53}=0.91$, $p=.35$, stimulus*group: $F_{1,53}=0.17$, $p=.68$). Adjusting for

the observed group differences at the end of extinction did not change the result (multiple regression including end-fear at extinction as well as fear acquisition and start-fear at extinction as covariates, non-preregistered analysis: spontaneous recovery: $\beta_{\text{group}}=.02$, $SE=.05$, $t_{40}=0.51$, $p=.61$; renewal: $\beta_{\text{group}}=.02$, $SE=.04$, $t_{40}=0.55$, $p=.58$; $n=45$), although it showed in both cases that end-fear at extinction significantly and positively predicted CRs at test (spontaneous recovery: $\beta_{\text{end-fear}}=.25$, $SE=.10$, $t_{40}=2.52$, $p=.02$; renewal: $\beta_{\text{end-fear}}=.27$, $SE=.09$, $t_{40}=3.06$, $p=.004$), as also observed in Gerlicher et al. (2018)¹⁶.

Since preregistration, three studies have reported that better extinction (lesser end-fear) is associated with better extinction retrieval in L-DOPA-treated, but not placebo-treated, participants, suggesting the L-DOPA effect may under some circumstances be restricted to successful extinguishers^{18,19}. However, in an additional non-preregistered interaction analysis, group did not interact with end-fear of extinction in predicting CRs at spontaneous recovery or renewal (all $p>.40$). Instead, comparable relationships between end-fear at extinction and CRs at the spontaneous recovery and renewal tests were found in both groups (simple slope analysis: spontaneous recovery: $\beta_{\text{end-fear/placebo}}=.24$, $SE=.13$, $t_{39}=1.86$, $p=.07$; $\beta_{\text{end-fear/L-DOPA}}=.26$, $SE=.16$, $t_{39}=1.65$, $p=.11$; renewal: $\beta_{\text{end-fear/placebo}}=.32$, $SE=.11$, $t_{39}=2.82$, $p=.008$; $\beta_{\text{end-fear/L-DOPA}}=.19$, $SE=.14$, $t_{39}=1.35$, $p=.19$; Fig. 2).

Together, these findings do not confirm an effect of L-DOPA on extinction memory consolidation but show a relationship between extinction success and extinction memory retrieval.

Relationship between vmPFC pattern reactivations post extinction and extinction memory retrieval

Next, we tested whether spontaneous post-extinction reactivations of a multi-voxel activity pattern (MVP) in the vmPFC, elicited by the offset of the first five CS+ trials early in extinction, on day 2 predict extinction memory retrieval at test on day 3 (preregistered hypothesis 2). We observed the predicted negative correlation between the number of vmPFC reactivations and

CRs in the spontaneous recovery test for the resting-state scan conducted 90 min after extinction ($\beta=-.10$, $SE=.03$, $t_{41}=3.17$, $p=.003$, $n=46$; Fig. 3), but not for the scans conducted 10 or 45 min after extinction ($p>.41$). Like in the discovery study, the relationship did not differ between groups (interaction number of reactivations at 90 min*group: $p=.66$, simple slope analysis: $\beta_{\text{placebo}}=-.09$, $p=.04$, $\beta_{\text{L-DOPA}}=-.12$, $p=.02$). The relationship did not extend to renewal (non-preregistered analysis, $p>.77$). Additional analyses confirmed the anatomical specificity of the relationship to the vmPFC (Supplementary Fig. 2).

Together, these results firmly establish an important role for spontaneous post-extinction reactivations of an extinction-related activity pattern in the vmPFC in the consolidation of long-term extinction memories.

Effect of L-DOPA administration post extinction on vmPFC reactivations

Next, we tested whether L-DOPA compared to placebo increases the number of spontaneous post-extinction vmPFC reactivations 10, 45, and 90 min after extinction (preregistered hypothesis 3). In congruence with an absent effect of L-DOPA on extinction retrieval, there was no observable effect of L-DOPA on the number of vmPFC reactivations during either of the resting-state scans (repeated-measures ANOVA: group: $p=.36$, time*group: $p=.70$, $n=46$; Fig. 4).

Together, these findings do not confirm an effect of L-DOPA on post-extinction vmPFC reactivations of an extinction-related activity pattern.

Relationship between salivary alpha-amylase and cortisol levels pre extinction with extinction memory retrieval, and interactions with L-DOPA administration post extinction

Our preregistered secondary research question 2 concerned whether individual differences in sAA and sCORT levels on the extinction day 2 had an influence on extinction memory retrieval

and might moderate the L-DOPA effect. To this aim we collected sAA and sCORT before and every 20 minutes after extinction on day 2 (Fig. 1c; for day 1 and 3 results, see Supplementary Fig. 3).

Time courses of both markers on day 2 exhibited linear decreases (effects of time: sAA: $F_{6,324}=9.50$, $p<.001$, $n=56$; sCORT: $F_{6,346}=27.45$, $p<.001$, $n=60$) in the absence of group influences (group and group*time: $p>.12$), with peak average levels of both sAA and sCORT observed before the start of the extinction session on day 2 (Fig. 5). Peak sAA and sCORT levels did not differ between groups (two-sample t-test: sAA: $t_{62}=0.31$, $p=.76$, $n=64$; sCORT: $t_{63}=0.42$, $p=.68$, $n=65$).

Pre-extinction sAA levels positively predicted CRs at spontaneous recovery ($\beta_{sAA}=.0007$, $SE=.0002$, $t_{45}=3.64$, $p<.001$, $n=49$). That is, higher arousal at the start of extinction appeared to be associated with relatively impaired extinction learning or consolidation (rather than with improved consolidation, as predicted by us²⁸). More intriguingly, when controlling for pre-extinction sAA, the analysis also showed an effect of L-DOPA ($\beta_{group}=.17$, $SE=.07$, $t_{45}=2.55$, $p=.01$) and a strong sAA by group interaction ($\beta_{sAA*group}=-.001$, $SE=.0003$, $t_{45}=3.37$, $p=.002$). See Fig. 5b,c. This means that controlling for acute arousal levels before extinction revealed a beneficial main effect of L-DOPA on extinction retrieval, and this L-DOPA effect was particularly pronounced at high levels of arousal. Whereas pre-extinction sAA positively predicted CRs at spontaneous recovery in the placebo group (Fig. 5b), a simple slope analysis showed an inversion of the sAA-to-spontaneous recovery relationship in the L-DOPA group ($\beta_{placebo}=.0007$, $p<.001$; $\beta_{L-DOPA}=-.0003$, $p=.18$, Fig. 5c). Hence, the analysis of sAA effects in our study suggests that arousal is an important moderator of dopaminergic extinction effects, as previously proposed^{18,19}. High arousal may thus be a necessary condition for extinction consolidation augmentation by L-DOPA.

A non-preregistered exploratory analysis further revealed that sAA levels before extinction were also associated at trend level with high extinction end-fear, that is, poor extinction

success ($\beta_{sAA}=.0004$, SE=.0003, $t_{42}=1.82$, $p=.08$; $\beta_{group}=-.13$, SE=.06, $t_{42}=2.10$, $p=.04$; $n=45$; Supplementary Fig. 4a). These results may support generally impairing effects of arousal on extinction, as suggested by animal studies³⁹, which in turn might be carried over to spontaneous recovery (see results above). There were no effects of sAA on extinction retrieval in the renewal test (non-preregistered exploratory analysis, not shown).

Pre-extinction sCORT also predicted CRs at spontaneous recovery, however, in the opposite direction (more sCORT – less spontaneous recovery; $\beta_{scort}=-.03$, SE=.01, $t_{46}=2.39$, $p=.02$; $n=50$; Supplementary Fig. 4b) and without influences of group ($p>.30$). Hence, the sCORT analyses only corroborate a previously reported positive influence of HPA axis activity on extinction consolidation^{35,40}, but do not speak for an interaction with dopamine levels.

sAA and sCORT originate from two different stress systems, the first being faster and more sensitive in responding to stressors, while the second responds more slowly and to more stressful tasks. Our current results suggest that acute arousal system activation (related to sAA) might have stronger direct effects on extinction than HPA system activation (related to sCORT) and show more important interactions with dopaminergic transmission.

Relationship between salivary alpha-amylase levels pre extinction with vmPFC reactivations during memory consolidation, and interaction with L-DOPA administration post extinction

As controlling for pre-extinction sAA in the present study had revealed the hypothesized beneficial effect of L-DOPA on extinction memory retrieval (which had not been found when testing for an L-DOPA effect alone), we generated the new hypothesis that controlling for pre-extinction sAA might also reveal a beneficial effect of L-DOPA on vmPFC reactivations 90 min after extinction. This non-preregistered exploratory analysis found a strong trend-wise main effect of group ($\beta_{group}=-.78$, SE=.39, $t_{49}=2.00$, $p=.05$, $n=53$), a weak trend-wise main effect of sAA ($\beta_{sAA}=-.002$, SE=.001, $t_{49}=1.82$, $p=.08$), and a significant sAA by group interaction

($\beta_{sAA*group}=.004$, $SE=.002$, $t_{49}=2.13$, $p=.04$). Simple slope analysis showed a tendency for a negative influence of pre-extinction sAA on vmPFC reactivations in the placebo group ($\beta_{placebo}=-.0019$, $p=.08$), in line with the above-reported negative association between sAA and extinction memory retrieval and with the trend-wise negative main effect of sAA found in this analysis. This negative sAA-to-vmPFC reactivations relationship was absent, and tended to be inversed, in the L-DOPA group ($\beta_{L-DOPA}=.0018$, $p=.20$; Fig. 6). That is, higher pre-extinction arousal was associated with fewer reactivations in the placebo, but not in the L-DOPA group. This latter result mirrors the result shown in Fig. 5b,c of an interaction between sAA and L-DOPA in their influence on spontaneous recovery.

The trend-wise main effect of group was negative, that is, there tended to be on average fewer activations in the L-DOPA relative to the placebo group after controlling for pre-extinction sAA levels. This further highlights the crucial importance of considering (nor)adrenaline or arousal levels when investigating L-DOPA effects on extinction consolidation, which should only be beneficial at high levels of arousal.

Neural correlates of salivary alpha-amylase levels pre extinction

sAA is only an indirect marker of (nor)adrenergic activity and arousal, and detection of alpha-amylase in saliva can be confounded by sources of bias and noise⁴¹. To corroborate the validity of sAA as a (nor)adrenergic marker, we performed a non-preregistered analysis asking whether pre-extinction sAA levels are associated with activity of a brain network anchored in the Locus coeruleus (LC), the major source of noradrenaline in the central nervous system and a key region of sympathetic control^{32,42}. In a first step, 35 brain regions exhibiting positive pre-extinction resting-state functional connectivity (FC) with the LC at $p<.001$ uncorrected were selected from an atlas-defined set of 436 cortical and subcortical regions (“LC network” (for details, see Methods). The data-driven selection mainly comprised prefrontal, thalamic, and striatal areas, the hypothalamus, and the dopaminergic midbrain (substantia nigra (SN), VTA). Using connectome-based predictive modeling (CPM⁴³), we found that FC within the LC

network (Fig. 7) was significantly associated with sAA values ($R=.32$, $p=.01$), while whole-brain FC or FC in a network anchored in dopaminergic midbrain areas (SN/VTA) was not (whole brain: $R=.01$, $p=.94$; SN/VTA: $R=.14$, $p=.28$). This suggests that our sAA values indeed reflect a functional activity state of the brain at the onset of extinction.

Discussion

The present study aimed to replicate the main study results of Gerlicher et al. (2018)¹⁶. We tested whether post-extinction L-DOPA as compared to placebo administration would improve extinction memory retrieval, as visible from reduced spontaneous recovery during an extinction memory test on day 3 of our experimental paradigm (hypothesis 1); whether the number of spontaneous reactivations of an extinction learning-related multi-voxel pattern (MVP) observed in the vmPFC in post-extinction resting-state scans would be predictive for extinction memory retrieval across treatment groups (hypothesis 2); and whether L-DOPA administration would relatively increase post-extinction vmPFC reactivations (hypothesis 3). The latter was done with an eye on potentially finding the mediation of the L-DOPA effect on retrieval by the increased number of vmPFC reactivations that was reported by Gerlicher et al. (2018)¹⁶. Two extensions further aimed at clarifying whether L-DOPA administration protects against the renewal of fear, tested on day 3 by presenting the CSs in a non-extinction context C (secondary research question 1), and whether peak sAA or sCORT levels on the extinction day 2 predict extinction memory retrieval on day 3 and interact with drug treatment in doing so (secondary research question 2).

We confirmed one of our three main hypotheses, namely that the number of spontaneous post-extinction reactivations of a vmPFC activity pattern observed during CS+ offsets in early extinction is predictive for extinction memory retrieval (hypothesis 2). Specifically, this was observed for the resting-state scan conducted 90 min after extinction. We could not replicate the facilitating effect of L-DOPA on extinction retrieval (hypothesis 1) and on the number of vmPFC reactivations (hypothesis 3). Examining whether L-DOPA could make extinction

memories context independent, we also did not find an advantage of L-DOPA administration for extinction memory retrieval in a renewal test (secondary research question 1). Collecting saliva samples at various time points to investigate the role of arousal and stress, we found that pre-extinction sAA was negatively, while pre-extinction sCORT was positively, associated with extinction memory retrieval. Further, sAA (but not sCORT) levels interacted with drug treatment in that the generally negative association of sAA with extinction retrieval (higher spontaneous recovery) was abolished in the L-DOPA group (secondary research question 2). Unexpectedly, the analysis also showed a beneficial main effect of L-DOPA on extinction retrieval. Hence, controlling for sAA levels at extinction onset revealed an L-DOPA effect that was not observable in the uncontrolled analysis conducted to test hypothesis 1.

We complemented these preregistered analyses with an exploratory analysis of L-DOPA effects on vmPFC reactivations 90 min after extinction that took into consideration pre-extinction sAA levels. sAA levels and L-DOPA treatment interacted in the sense that sAA tended to be negatively related with the number of vmPFC reactivations in the placebo group, but positively in the L-DOPA group.

Our main replication finding is that spontaneous post-extinction reactivations of a CS+ offset-related vmPFC activity pattern positively associate with later extinction memory retrieval. This result is in line with previous animal research, showing that spontaneous IL activity after extinction learning is crucial for consolidation and predictive for memory retrieval⁴⁴. Additionally, stimulus-specific fMRI multi-voxel reactivation patterns in other learning domains and brain regions also have been reported to be associated with later memory performance outcomes⁴⁵. The reactivation pattern in our work specifically recapitulates CS+ offset-related activity in the vmPFC during *early* extinction. The CS+ offset is the time point in a trial at which participants have learned to expect a US during prior conditioning, and the omission of the US that occurs during the extinction phase is most unexpected at the beginning of extinction, while less of a surprise at later extinction trials. This suggests that the vmPFC may reactivate a prediction error (PE) signal, which learning theory considers to be the key teaching signal in

associative learning^{22,46}. In extinction specifically, the PE may not so much lead to an update (reduction) of the aversive value of the CS, but rather to the build-up of a new, appetitive safety memory (a CS–noUS association, or extinction memory) that antagonistically inhibits the CS–US association (or fear memory)^{47,48}. On this basis, one can postulate that vmPFC reactivations of important extinction learning events after extinction provide the link between extinction learning and extinction memory retrieval, by facilitating the storage and consolidation of a safety association.

One open question is why we find a predictive effect of vmPFC reactivations for memory retrieval at 90 min after extinction and not at 45 min, as in the discovery study. Animal studies indicate that the time window for consolidation processes can be broad, spanning hours and even extending into sleep, depending on which molecular or network mechanisms are involved⁴⁹. Further, while molecular consolidation processes are bound to specific timelines⁵⁰, they may still show substantial interindividual differences, for instance, due to differences in the speed or success of learning, in the individual make-up of the molecular systems, or in the current state of the system in which a consolidation process occurs (e.g., in stress, vigilance, arousal etc.). Such differences have not been explored in human work but may lead to substantial heterogeneity in consolidation dynamics across studies.

Previous studies from our group using a cue conditioning and extinction paradigm have reported pronounced L-DOPA main effects when experiments were conducted in MRI^{14,16}, but only conditional L-DOPA effects (in participants with successful extinction learning) when experiments were purely behavioral (two experiments¹⁸). Because there is evidence that the scanner environment is frequently perceived by participants as arousing and stressful^{36–38}, this pattern of results prompted us to postulate that L-DOPA might be more effective in promoting extinction memory consolidation under conditions of high arousal and/or stress, as apparent from high sAA or sCORT levels²⁸.

We observed that higher sAA levels at extinction onset were associated with fewer post-extinction vmPFC reactivations and worse extinction retrieval, and that these effects were rescued by L-DOPA administration after extinction. We also observed a beneficial L-DOPA main effect on retrieval in the analysis that controlled for sAA levels. These findings indeed suggest that L-DOPA is more effective when extinction has occurred in a highly aroused state. From a clinical point of view, this may be very good news for a potential application of L-DOPA as a pharmacological augmentation of exposure-based therapy⁹, since exposure is typically accompanied by high fear and arousal. From a scientific point of view, we may have identified an important individual-differences factor that should be considered in future studies testing methods to optimize extinction or exposure therapy – via L-DOPA and potentially also via other routes.

Mechanistically, a simple explanation for a better efficacy of L-DOPA at high arousal states may be that L-DOPA has more room to improve extinction consolidation when it is compromised by (nor)adrenergic activity. Alternatively, L-DOPA may also directly interfere with the impairing effects of central noradrenaline on extinction consolidation. Previous research has suggested that, at high arousal levels, noradrenaline released from LC projections in the basolateral amygdala (BLA) acts via α 1- and β -adrenoceptors to increase BLA activity, while noradrenaline release in the mPFC reduces activity there. Further, the increased BLA activity also attenuates mPFC output via inhibitory BLA-mPFC projections. In sum, there is an increase in fear and impeded learning and/or consolidation^{33,39}. Dopamine may counteract these impairing effects of noradrenergic activity, first, by decreasing prefrontal extracellular noradrenaline levels via increased neuronal reuptake and activation of inhibitory α 2-adrenoceptors¹³, and second, by directly reducing BLA-mediated inhibition of the mPFC⁵¹. Together, these findings point to a possible mechanism by which systemic L-DOPA administration abolishes the detrimental high-arousal effects on extinction learning and consolidation. Therefore, it is well conceivable that administering L-DOPA as an adjunct to exposure treatments in clinical practice might exert beneficial effects, as high systemic arousal

is a likely feature of exposure. Further investigation is needed to replicate the current findings of an interaction between arousal and dopaminergic activity in humans in shaping extinction memory consolidation. Importantly, future work should also experimentally manipulate the arousal system.

In this replication study, we aimed at reproducing the main findings from Gerlicher et al. (2018)¹⁶ with minor extensions. Our results firmly establish the predictive role of a potentially PE-related reactivation pattern in the vmPFC for extinction memory retrieval, tested in spontaneous recovery. We discover that high arousal in humans is associated with impaired extinction consolidation and that L-DOPA promotes extinction consolidation specifically under conditions of high arousal. This result opens up new avenues for the investigation of L-DOPA as an enhancer of exposure therapy. For fear extinction research, our results lead to new mechanistic hypotheses and suggest a new possibility to explain the vast individual differences frequently observed in human extinction research.

Methods

Design. The study design is as in the discovery study, with the exception of the added sAA and sCORT measurements on days 1 and 2 and the added renewal test on day 3.

Sample size. Our major effect of interest in the discovery study¹⁶ was the interaction effect of stimuli (CS+/CS-) and group (placebo/L-DOPA) on average SCRs during the test in the extinction context on day 3, corresponding to our replication hypothesis 1. This effect had a size of $\eta_p^2=.166$, calculated by IBM SPSS Statistics (version 23, Chicago IL). Using this effect size, we estimated using G*power 3.1.9.2⁵² that with a power of 80% and an alpha of 0.05, the required sample size would be N=22, i.e., n=11 participants per group. As stated in the Introduction, further statistical, logistical, and ethical considerations led us to aim at a sample size of N=63 after drop-outs, requiring us to recruit 70 participants. Supplementary Table 1 gives demographic information and further characteristics of the full recruited sample.

Technical problems in data acquisition, described below for each data modality in the corresponding Methods sections, reduced sample sizes for the analysis of the data modalities. Supplementary Table 2 lists the missing data per participant, data modality, and day. The final n for each analysis is indicated in the corresponding sections of the Results. For the testing of our main hypothesis 1, using SCR data, we achieved a final n of 55, which is 1.4 times greater than the discovery sample and 2.5 times greater than the critical sample size estimated based on power calculation. This suggests that the null finding in the analysis testing hypothesis 1 is not due to insufficient power.

Participants. As in the discovery study, we restricted recruitment to male participants. The estrous cycle has been shown to interact with extinction memory consolidation^{53,54}, and dopamine has been shown to have opposing effects on extinction depending on estrous cycle phase⁵⁵. Thus, by limiting ourselves to male participants, we could expect higher sample homogeneity and correspondingly higher chances for detecting a neurobiological mechanism. After safely demonstrating an effect with this strategy, a necessary next step is to test transfer to non-male populations. A board-certified physician screened participants for contraindications of L-DOPA intake, current physiological, neurological, or psychiatric disorders, excessive consumption of nicotine (>10 cigarettes/day), alcohol (>15 glasses of beer/wine per week), or cannabis (>1 joint/month), participation in other pharmacological studies, and skin conductance non-responding (assessed by eSense Skin response, Mindfield® Biosystems Ltd., Berlin, Germany). Drug abuse was assessed via a urine test (M-10/3DT; Diagnostik Nord, Schwerin, Germany). The experiment was approved by the local ethics committee (Ethikkommission der Landesärztekammer, Rhineland-Palatinate, Germany) and was conducted in accordance with the Declaration of Helsinki.

Experimental Design. We used a three-day fear conditioning and extinction paradigm consisting of conditioning (day 1) in context A, extinction (day 2) in context B, and tests for the effect of L-DOPA on extinction memory retrieval in the original extinction context (B) and in a new context (C) (day 3). See Fig. 1a. Our study involves a 2x2 mixed factorial design with

stimulus as within- (CS+ vs. CS-) and drug group as between-subject (placebo vs. L-DOPA) factor. As in our previous studies^{14,16,18,19}, the main outcome measures were average CS evoked SCRs during each of the test contexts on day 3.

Stimuli. Two black geometric symbols (a square and a rhombus) presented in the center of the screen served as CSs. The symbols were super-imposed on background pictures of one of three different gray photos (living room, kitchen, and sleeping room), which served as contexts A, B, and C. The assignment of symbols to the CS+ and CS- and backgrounds to the conditioning, extinction or renewal context were randomized between participants and groups. Diminishing the risk of low-visual feature differences between the CS+ and the CS-, contrast and luminance of stimuli were adjusted using SHINE toolbox⁵⁶. Stimuli were presented using Presentation Software (Presentation®, Neurobehavioral Systems, Inc., Berkeley, CA, USA). A painful electrical stimulation consisting of three square-wave pulses of 2 ms (50 ms inter-stimulus interval) was employed as US. Pain stimuli were generated by using a DS7A electrical stimulator (Digitimer, Weybridge) and delivered to the skin through a surface electrode with a platinum pin (Specialty Developments, Bexley, UK). Due to observed incidences of high-voltage MRI artefacts in previous studies, we moved the stimulation further away from the magnet's bore from the dorsal hand (pre-registered location of stimulation) to the ankle.

Drug treatment. Participants were randomly assigned to the L-DOPA or the placebo group using a randomization list generated before the start of the study, with the restriction that groups had to be matched on self-reported trait anxiety based on the State-Trait Anxiety Inventory questionnaire (STAI-T⁵⁷). STAI-T scores did not differ between groups after acquisition of n=45 participants, and therefore the predefined treatment group randomization order was kept. After full data acquisition, STAI-T values did not differ between groups (Supplementary Table 1). Other than in Gerlicher et al. (2018)¹⁶ and than preregistered²⁸, anxiety sensitivity index (ASI) scores, originally intended to also be matched between groups, were not acquired due to an initially undetected technical failure. Drug preparation was done

by a person not involved in the experiments or analyses. Participants were administered either 150/37.5 mg L- DOPA-benserazide (Levodopa-Benserazid-ratiopharm®, Germany; for dosage see^{14,17}) or a visually identical capsule filled with mannitol and aerosil (i.e. placebo). Drugs were prepared and provided by the pharmacy of the University Medical Center Mainz and administered in a double-blind fashion. Participants were asked to refrain from eating, consuming caffeinated drinks, and smoking two hours prior to drug intake. Fasting L-DOPA absorption is rapid, with L-DOPA peak plasma concentration reaching within 15 to 60 min after oral intake⁵⁸. Furthermore, L-DOPA half-time is also short (90 minutes), excluding that drug effects on extinction retrieval can be explained by direct drug action on the test day.

Experimental procedures

Day 1 - fear learning. Participants filled out the state version of the state-trait anxiety inventory (STAI-S), the Acceptance and Action questionnaire (AAQ⁵⁹) the General Health Questionnaire (GHQ⁶⁰) (no group differences in all questionnaires; for analyses, see Supplementary Table 1) and answered a list of questions assessing behaviors potentially influencing on sCORT measurements (no group differences in all measures; for analyses, see Supplementary Table 3). Subsequently, a saliva sample was collected. Participants were placed in the MRI scanner, and SCR and pain stimulation electrodes were attached. An 8-min resting-state scan was conducted. Participants then were familiarized with the experiment through two CS presentations in each of the three contexts and a training of US-expectancy ratings (for analyses, see Supplementary Fig 1). US-expectancy ratings were taken on all three days as additional check for the success of conditioning, extinction, and extinction retrieval, respectively. Subsequently, US-intensity was calibrated to a level rated as “maximally painful, but still tolerable” (for analyses, see Supplementary Table 1). Participants were then instructed that one symbol would never be followed by a pain stimulus and that their task was to find out what rule applied to the other symbol. After scanning onset, the paradigm started with US-expectancy ratings for each CS. After the initial rating, a background picture representing context A appeared on the screen. The context picture remained on the screen continuously

throughout conditioning. Participants were presented with 10 CS+ and 10 CS- trials. Notably, 5 out of 10 CS+ presentations (i.e., 50%) were reinforced. CSs were presented for 4.5 seconds. In case of reinforced CS+ presentations, the US was delivered such that it co-terminated with the CS presentation. Inter-trial intervals (ITIs) lasted 17, 18, or 19 seconds. Trial order was randomized in such a way that not more than two trials of the same type (i.e., CS+ with US, CS+ without US, CS-) succeed each other. Conditioning lasted approximately 12 min and scanning ended after picture offset and US-expectancy ratings. After conditioning, another 8-min resting-state scan was conducted, followed by anatomical scans (T1, T2, DTI, see Acquisition of MRI data). Subsequently, electrodes were detached, participants gave another saliva sample and filled out a list of questions assessing contingency knowledge (for details, see Supplementary Methods). The whole procedure lasted approximately 90 min.

Day 2 - Extinction learning and consolidation. After 24 h (± 2 h), participants came back to the laboratory to fill out the STAI-S questionnaire and answer questions on behaviors potentially influencing sCORT measures. Participants provided a saliva sample and were placed in the scanner. Electrodes were attached, and participants were instructed that the experiment would continue, and that their individual US strength from day 1 would be applied. An 8-min resting-state scan was conducted. Before and after extinction, US-expectancy ratings were taken. During extinction, a background picture representing context B was continuously shown on the screen and participants were presented 15 CS+ and CS- trials, using the same timings and pseudo-randomization algorithm as in conditioning. Extinction lasted approximately 15 min. Subsequently, participants were taken out of the scanner for saliva sample collection, detaching of electrodes and receiving either a placebo or L-DOPA pill. Participants stayed under observation for 90 minutes. During this period, further 8-min resting-state scans were performed ~10, 45, and 90 minutes after extinction end, and saliva samples were collected each 20 min starting from the saliva collection time point at extinction end (see Fig. 1c). Before leaving the laboratory, participants filled out the STAI-S, a list of questions assessing contingency knowledge and a questionnaire assessing possible side-

effects of L-DOPA intake (for details, see Supplementary Table 4). The whole procedure lasted approximately 150 min.

Day 3 – Extinction memory retrieval test (spontaneous recovery and renewal). After 24 h (± 2 h), participants came back to the laboratory and filled out the STAI-S and side-effects questionnaires and answered questions regarding potential confounding factors on sCORT measurements. Participants provided a saliva sample and were placed in the scanner, electrodes were attached, and participants were instructed that their US strength from day 1 would be applied and that the experiment would continue. An 8-min resting-state scan was conducted. Before and after the test, US-expectancy ratings were taken. During the test, participants were then presented 10 CS+ and 10 CS- trials in context B first (spontaneous recovery test) and subsequently the same number of trials in context C (renewal test), applying timings and randomization as on day 1. Finally, another saliva sample was taken, and participants filled out a questionnaire assessing contingency knowledge. The test lasted about 20 min; the whole procedure lasted approximately 60 min.

Skin conductance responses (SCRs). CS elicited SCRs were employed as conditioned fear responses (CRs). Electrodermal activity was recorded from the thenar and hypo-thenar of the non-dominant hand using self-adhesive Ag/AgCl electrodes pre-filled with an isotonic electrolyte medium and the Biopac MP150 with EDA100C device (EL-507, BIOPAC® Systems Inc., Goleta, California, USA). The raw signal was amplified and low-pass filtered with a cut-off frequency of 1 Hz. The onset of SCRs was visually scored offline in a time window from 900 to 4000 ms after CS onset. The phasic amplitude of SCRs was calculated by subtracting the onset background tonic skin conductance level (SCL) from the subsequent peak, using a custom-made analysis script. Technical problems in data acquisition led to missing data in $n=0/3/3$ participants for days 1/2/3, respectively. SCRs with amplitudes smaller than 0.02 μ s were scored as zero and remained in the analysis. If more than 75% of trials during an experimental session were scored as zero, data of this participant during that session was regarded as invalid and excluded from SCR analysis ($n=4/16/12$ on days 1/2/3). Hence, in

total, data from n=4/19/15 participants on days 1/2/3 were not available for analysis. To normalize distributions, data was log-transformed (+1 and log) and range-corrected for each participant and experimental session (i.e., $(\text{SCR} - \text{SCRmin}) / \text{SCRmax}^{61}$).

Heart rate. Heart rate was recorded with an MRI-compatible fibre-optic pulse oximeter during both resting-state scans and experimental sessions. We assessed heart rate during the resting-state phases preceding each experimental session as an indicator of autonomic stress response. Further analyses were not implemented, as data was largely lost due to a storage error.

Pupil dilation. Pupil dilation was assessed monocularly using an MRI-compatible camera (MR Cam Model 12M; MRC systems, Germany). The iViewX 2.8 software (Sensormotoric Instruments, Germany) was used for recordings. Contrary to our pre-registration, no analyses were conducted, as data was largely incomplete due to technical camera problems.

US-expectancy ratings. Participants were asked to indicate the expectancy of receiving an electric pain stimulation for each CS with a cursor on a visual analogue scale from 0 = “no expectancy” to 100 = “high expectancy”. The start position of the cursor on the scale was determined randomly. Ratings were not available for n=0/3/3 participants on days 1/2/3. According to the ratings, participants showed successful fear acquisition, extinction, and extinction memory retrieval. For results, see Supplementary Fig 1.

Salivary alpha-amylase and cortisol measurement. Saliva samples were collected from the participants outside the scanner using cotton swabs. Samples were taken before and after the fMRI scan on days 1 and 3. On day 2, the saliva samples were collected before and after the first fMRI scan. Five additional saliva samples were collected approximately every 20 minutes after extinction learning (total n=11, Fig 1c for day 2 timeline). Immediately after taking the samples, saliva was stored at -20 °C until assayed. sCORT and sAA were determined using a commercial enzyme immunoassay, see Supplementary Methods. Data was missing due to lack of saliva, or incomplete due to insufficient saliva for more than one measure from

one swab, that is, sCORT was measured first, and no more saliva was left for the sAA measurement (missing values: sCORT: n=4 on day 1, n=5 on day 2 pre extinction, n=11 of six swab times post extinction, n=10 on day 3; sAA: n=9 on day 1, n=6 on day 2 pre extinction, n=14 of six swab times post extinction, n=14 on day 3).

Acquisition of MRI data. MRI data was acquired on a Siemens MAGNETOM Trio 3 Tesla MRI System using a 32-channel head coil. Resting-state and task data were recorded using gradient echo, echo planar imaging (EPI) with a multiband sequence covering the whole brain (TR: 1000 ms, TE: 29 ms, multi-band acceleration factor: 4, voxel-size: 2.5 mm isotropic, flip angle 56°, field of view: 210 mm;⁶²). A high-resolution T1 weighted image was acquired after the experiment on day 1 for anatomical visualization and normalization of the EPI data (TR: 1900 ms, TE: 2540 ms, voxel size: 0.8 mm isotropic, flip angle 9°, field of view: 260 mm, MPRAGE sequence). T2 weighted images were collected for preventative neuro-radiological diagnostics for all participants (45 slices, TR: 6100 ms, TE: 79 ms, voxel size: 3 mm isotropic, flip angle: 120°, Turbo Spin Echo (TSE) sequence). Lastly, we collected multidimensional diffusion-weighted tensor images (DTI) from each participant (72 slices, voxel-size: 2 mm isotropic, TR: 9100 ms, TE: 85 ms, number of directions: 64, diffusion weights: 2, *b*-value 1: 0 s/mm², *b*-value 2: 1000 s/mm², Multi-Directional Diffusion Weighted (MDDW) sequence)).

For the acquisition of the resting-state scans, participants were instructed to remain awake, keep their eyes open, fixate a black cross presented in the center of a grey screen, and let their mind wander freely. Compliance with the instruction to remain awake was monitored online using video recordings of the right eye. After each resting-state scan, participants rated their tiredness on a scale from 0 = “not tired at all” to 100 = “almost fell asleep” (for analyses, see Supplementary Table 1). No resting-state data had to be excluded due to sleep.

MRI data were not available due to technical problems from n=0/3/3 participants on days 1/2/3.

Preprocessing of fMRI data. Only task and resting-state fMRI data from day 2, relevant to address our hypotheses, were analyzed and are reported here. fMRI data was preprocessed

and analyzed using statistical parametric mapping (SPM12, Wellcome Trust Centre for Neuroimaging, London, UK, <http://www.fil.ion.ucl.ac.uk/>) running on Matlab 2015b (MathWorks®, Natick, Massachusetts, USA). The first 5 volumes of each scan were discarded due to equilibrium effects. Preprocessing includes realignment and co-registration of the mean functional image to the T1 weighted anatomical image. Subsequently, the T1 weighted anatomical image was segmented and normalized to add Montreal Neurological Institute (MNI) space based on SPM's tissue probability maps. Normalization of the functional images was achieved by applying the resulting deformation fields to the realigned and co-registered functional images. Lastly, functional data was smoothed using a 6mm full-width-at-half-maximum Gaussian smoothing kernel. Data of participants was excluded when movement peaks exceeded more than 3 mm or 2° (task data, n=7, resting-state data: n=6 further participants).

Data analysis

Statistical analysis of behavioral and psychophysiological data. For statistical analysis of SCR and US-expectancy ratings, we conducted repeated measures ANOVA with stimulus (CS+/CS-) as within- and drug (placebo/L-DOPA) as between-subject factor. Following our previous studies^{16,18,19} and preregistration, we tested whether fear was successfully acquired based on CRs averaged across the last 20% of trials during fear conditioning (i.e., last 2 trials). Start-fear at extinction on day 2 was assessed using the average first 20% of trials during extinction (i.e., first 3 trials). End-fear of extinction was determined across the last 20% of trials (i.e., last 3 trials) of the extinction session on day 2. The effect of L-DOPA on retrieval was tested using CRs averaged across all trials of either the spontaneous recovery or the renewal test on day 3.

Multivariate fMRI analysis. Investigating potential reactivations of extinction specific MVPs in the vmPFC, we analyzed the extinction task data (day 2) using a model including one regressor for CS+ and CS- onsets, respectively, US-expectancy ratings, and context on/-

offset. Furthermore, the model included one regressor for the first five CS+ offsets, where omission of the US was unexpected, and one for the first five CS- offsets, where US omission was expected, as well as one regressor each for the remaining ten CS+ and CS- offsets. All regressors were delta-functions convolved with the hemodynamic response function (HRF). The MVP evoked by the first five US omissions at CS+ offset in the vmPFC was extracted from the resulting beta-map in the vmPFC region of interest (ROI; see below). Resting-state data was analyzed in accordance with a previous study examining memory reactivation⁶³ (see also¹⁶), i.e., general linear models (GLMs) for each day 2 resting-state scan (pre-, ~10, 45 and 90 minutes post-extinction) included delta-function regressors for each volume (TR: 1 sec), thereby accounting for potential reactivations which may have occurred during any point of the resting-state scan. No high-pass filtering was applied in the resting-state models and AR(1) auto-correlation correction was employed. MVPs in the pre-defined ROI during the resting state were extracted from the resulting beta-image series (TR = 1 second, i.e., 480 – 5 = 475 beta images).

Subsequently, we correlated (Pearson correlation coefficient) the pattern evoked by the first five US omissions at CS+ offset during extinction with the resulting 475 patterns of all four resting-state scans and Fisher Z- transformed the correlation coefficients. The 475 correlations of the US omission pattern with the resting-state pattern recorded before extinction learning was employed to create a baseline distribution. The mean and standard deviation of this baseline distribution was used to transform each correlation between the template and the resting-state patterns into a Z- score ($Z_i = (r_i - \mu_i)/\sigma$). Correlations with a Z-score exceeding a value of 2 ($Z > 2 \approx p < .05$) were counted as potential reactivations of the CS+ offset-related vmPFC pattern. Reactivations were summed per participant and resting-state scan. Subsequently, multiple linear regression analyses with number of CS+ offset-related vmPFC reactivations at baseline, ~10, 45, and 90 min after extinction as predictors and average differential (CS+>CS-) SCR during either the spontaneous recovery or the renewal test as dependent variables were performed separately.

Regions of interest (ROIs). We focused our analysis on the vmPFC based on previous work¹⁶. Control regions involved in fear and extinction learning were included comprising of: anterior cingulate cortex (ACC), superior frontal gyrus (SFG), left and right insula, left and right amygdala, and left and right hippocampus (see Supplementary Fig. 2 for results). All ROIs were extracted from the Harvard-Oxford Atlas and thresholded at 50%-tissue probability by previous work¹⁶.

Locus coeruleus network analysis

To examine whether sAA levels can be linked to the inherent activity of the locus coeruleus (LC) network, we employed a customized resting-state fMRI data analysis pipeline implemented in Python (3.9.2), which requires the data to be preprocessed by fMRIPrep (for a complete fMRIPrep report see Supplementary Methods). After fMRIPrep of the baseline resting-state scan on day 2, three participants were excluded due to motion artifacts (framewise displacement > 3mm) and one participant because fMRIPrep returned an erroneous T1-to-MNI transform (n=66). Denoising included detrending, band-pass filtering (0.01-0.1 Hz) and 4mm gaussian smoothing. Mean white matter (WM) and cerebrospinal fluid (CSF) time courses as well as motion parameters and their first derivatives were regressed out. The first four images were removed prior to data analysis. Subject-wise whole-brain functional connectivity (FC, defined as Pearson's correlation coefficients) matrices were created based on a combined set of atlases comprising 436 cortical and subcortical brain regions (see Supplementary Methods). FC scores were Fisher Z-transformed and brain regions showing high FC scores with the LC ($p < .001$ uncorrected) were defined as LC network nodes. For each participant, an FC matrix comprising FC scores between LC network nodes was created and used as input for connectome-based predictive modeling (CPM) to predict individual sAA levels⁴³. Unlike the rest of the pipeline, CPM was performed in Matlab (versionR2017b). As sAA values of five further participants were missing, CPM was performed on n=61 participants. In CPM, edges of the input matrices (here LC network matrices) are first correlated with the behavioral/physiological measure of interest (here sAA values), and those

edges showing significant positive or negative correlations ($p < .05$) are selected (here only positive correlations were considered). In a leave-one-out cross-validation, a single summary statistic is calculated for $n-1$ participants by adding up FC values of the selected edges. These summary statistics were entered in a GLM to test the relationship with sAA values. True sAA values of the left-out participants were then correlated with sAA values predicted by the GLM to evaluate the predictive power (for more details on CPM, see⁶⁴).

Acknowledgments

This work was funded by the Deutsche Forschungsgemeinschaft (DFG), SFB1193, subproject C01 to R.K.

Author contributions

E.A., C.-P.H., A.M.V., O.T. and R.K. designed the experiment; E.A. and C.-P.H. collected the data; E.A., C.-P.H., and B.M. analyzed the data; and E.A. and R.K. wrote the paper.

Competing interests

R.K. has received advisory honoraria from JoyVentures, Herzlia, Israel.

References

1. Zuj, D. V., Palmer, M. A., Lommen, M. J. J. & Felmingham, K. L. The centrality of fear extinction in linking risk factors to PTSD: a narrative review. *Neurosci. Biobehav. Rev.* **69**, 15–35 (2016).
2. Craske, M. G., Hermans, D. & Vervliet, B. State-of-the-art and future directions for extinction as a translational model for fear and anxiety. *Philos. Trans. R. Soc. B Biol. Sci.* **373**, (2018).
3. Vervliet, B., Craske, M. G. & Hermans, D. Fear extinction and relapse: state of the art. *Annu. Rev. Clin. Psychol.* **9**, 215–248 (2013).
4. Pavlov, I. P. Conditioned reflexes. An investigation of the physiological activity of the cerebral cortex. *Oxford Univ. Press* (1927) doi:10.2307/1134737.
5. Bouton, M. E. Context and behavioral processes in extinction. *Learn. Mem.* **11**, 485–494 (2004).
6. Müller, G. E. & Pilzecker, A. *Experimentelle Beiträge zur Lehre vom Gedächtnis. Z. Psychol. Ergänzungsband* 1–300 (1900).
7. Nadel, L. & Moscovitch, M. Memory consolidation, retrograde amnesia and the hippocampal complex. *Curr. Opin. Neurobiol.* **7**, 217–227 (1997).
8. Squire, L. R. Mechanisms of Memory. *Science*. **232**, 1612–1619 (1986).
9. Singewald, N., Schmuckermair, C., Whittle, N., Holmes, A. & Ressler, K. J. Pharmacology of cognitive enhancers for exposure-based therapy of fear, anxiety and trauma-related disorders. *Pharmacol. Ther.* **149**, 150–190 (2015).
10. Iemolo, A., De Risi, M. & De Leonibus, E. *Role of Dopamine in Memory Consolidation. Sakakibara, M and Ito E eds. Memory Consolidation. Nova Science Publisher* (2015).
11. Hikind, N. & Maroun, M. Microinfusion of the D1 receptor antagonist, SCH23390 into the IL but not the BLA impairs consolidation of extinction of auditory fear conditioning. *Neurobiol. Learn. Mem.* **90**, 217–222 (2008).
12. Abraham, A. D., Cunningham, C. L. & Lattal, K. M. Methylphenidate enhances extinction of contextual fear. *Learn. Mem.* **19**, 67–72 (2012).
13. Dayan, L. & Finberg, J. P. M. L-DOPA increases noradrenaline turnover in central and peripheral nervous systems. *Neuropharmacology* **45**, 524–533 (2003).
14. Haaker, J. *et al.* Single dose of L-dopa makes extinction memories context-independent and prevents the return of fear. *Proc. Natl. Acad. Sci. USA* **110**, E2428–E2436 (2013).
15. Whittle, N. *et al.* Enhancing dopaminergic signaling and histone acetylation promotes long-term rescue of deficient fear extinction. *Transl. Psychiatry* **6**, (2016).
16. Gerlicher, A. M. V., Tüscher, O. & Kalisch, R. Dopamine-dependent prefrontal reactivations explain long-term benefit of fear extinction. *Nat. Commun.* **9**, 4294 (2018).
17. Haaker, J., Lonsdorf, T. B. & Kalisch, R. Effects of post-extinction L-DOPA administration on the spontaneous recovery and reinstatement of fear in a human fMRI study. *Eur.*

Neuropsychopharmacol. **25**, 1544–1555 (2015).

- 18. Gerlicher, A. M. V., Tüscher, O. & Kalisch, R. L-DOPA improves extinction memory retrieval after successful fear extinction. *Psychopharmacology (Berl.)*. (2019) doi:10.1007/s00213-019-05301-4.
- 19. Gerlicher, A. M. V., Ilhan-Bayrakci, M., Tüscher, O. & Kalisch, R. Post-extinction L-DOPA administration to reduce the return of fear in humans. *PsyArXiv Prepr.* (2022) doi:10.31234/osf.io/rhnsa.
- 20. Milad, M. R. & Quirk, G. J. Fear extinction as a model for translational neuroscience: ten years of progress. *Annu. Rev. Psychol.* **63**, 129–151 (2012).
- 21. Hugues, S., Garcia, R. & Léna, I. Time course of extracellular catecholamine and glutamate levels in the rat medial prefrontal cortex during and after extinction of conditioned fear. *Synapse* **61**, 933–937 (2007).
- 22. Rescorla, R. A. & Wagner, A. R. A theory of pavlovian conditioning: variations in the effectiveness of reinforcement and nonreinforcement. *Class. Cond. II Curr. Res. theory* 64–99 (1972) doi:10.1101/gr.110528.110.
- 23. Pearce, J. M. & Hall, G. A model for pavlovian learning: variations in the effectiveness of conditioned but not of unconditioned stimuli. *Psychol. Rev.* **87**, 532–552 (1980).
- 24. Dunsmoor, J. E., Niv, Y., Daw, N. & Phelps, E. A. Rethinking extinction. *Neuron* **88**, 47–63 (2015).
- 25. Papalini, S., Beckers, T. & Vervliet, B. Dopamine: from prediction error to psychotherapy. *Transl. Psychiatry* **10**, 164 (2020).
- 26. Kalisch, R., Gerlicher, A. M. V. & Duvarci, S. A dopaminergic basis for fear extinction. *Trends Cogn. Sci.* **23**, 274–277 (2019).
- 27. Thiele, M., Yuen, K. S. L., Gerlicher, A. V. M. & Kalisch, R. A ventral striatal prediction error signal in human fear extinction learning. *Neuroimage* **229**, 117709 (2021).
- 28. Chuan-Peng, H. *et al.* Dopamine-dependent prefrontal reactivations explain long-term benefit of fear extinction: A direct replication attempt. *osf.io/x64cn* (2018).
- 29. Simonsohn, U. Small telescopes: detectability and the evaluation of replication results. *Psychol. Sci.* **26**, 559–569 (2015).
- 30. Bacchetti, P., Wolf, L. E., Segal, M. R. & McCulloch, C. E. Ethics and sample size. *Am. J. Epidemiol.* **161**, 105–110 (2005).
- 31. Kirschbaum, C. & Hellhammer, D. H. Salivary cortisol in psychobiological research: an overview. *Neuropsychobiology* **22**, 150–169 (1989).
- 32. Nater, U. M. & Rohleder, N. Salivary alpha-amylase as a non-invasive biomarker for the sympathetic nervous system: current state of research. *Psychoneuroendocrinology* **34**, 486–496 (2009).

33. Giustino, T. F. & Maren, S. Noradrenergic modulation of fear conditioning and extinction. *Front. Behav. Neurosci.* **12**, 1–20 (2018).
34. Joëls, M., Pu, Z., Wiegert, O., Oitzl, M. S. & Krugers, H. J. Learning under stress: how does it work? *Trends Cogn. Sci.* **10**, 152–158 (2006).
35. Meir Drexler, S., Merz, C. J., Jentsch, V. L. & Wolf, O. T. Stress modulation of fear and extinction in psychopathology and treatment. *Neuroforum* **26**, 133–141 (2020).
36. Muehlhan, M., Lueken, U., Wittchen, H. U. & Kirschbaum, C. The scanner as a stressor: Evidence from subjective and neuroendocrine stress parameters in the time course of a functional magnetic resonance imaging session. *Int. J. Psychophysiol.* **79**, 118–126 (2011).
37. Visser, R. M., Kunze, A. E., Westhoff, B., Scholte, H. S. & Kindt, M. Representational similarity analysis offers a preview of the noradrenergic modulation of long-term fear memory at the time of encoding. *Psychoneuroendocrinology* **55**, 8–20 (2015).
38. Eatough, E. M., Shirtcliff, E. A., Hanson, J. L. & Pollak, S. D. Hormonal reactivity to MRI scanning in adolescents. *Psychoneuroendocrinology* **34**, 1242–1246 (2009).
39. Maren, S. Unrelenting Fear Under Stress: Neural circuits and mechanisms for the immediate extinction deficit. *Front. Syst. Neurosci.* **16**, 1–13 (2022).
40. Ninomiya, E. M. *et al.* Spironolactone and low-dose dexamethasone enhance extinction of contextual fear conditioning. *Prog. Neuro-Psychopharmacology Biol. Psychiatry* **34**, 1229–1235 (2010).
41. Ali, N. & Nater, U. M. Salivary alpha-amylase as a biomarker of stress in behavioral medicine. *Int. J. Behav. Med.* **27**, 337–342 (2020).
42. Morris, L. S., McCall, J. G., Charney, D. S. & Murrough, J. W. The role of the locus coeruleus in the generation of pathological anxiety. *Brain Neurosci. Adv.* **4**, 239821282093032 (2020).
43. Rosenberg, M. D., Finn, E. S., Scheinost, D., Constable, R. T. & Chun, M. M. Characterizing attention with predictive network models. *Trends Cogn. Sci.* **21**, 290–302 (2017).
44. Burgos-Robles, A., Vidal-Gonzalez, I., Santini, E. & Quirk, G. J. Consolidation of fear extinction requires NMDA receptor-dependent bursting in the ventromedial prefrontal cortex. *Neuron* **53**, 871–880 (2007).
45. Tambini, A. & Davachi, L. Awake reactivation of prior experiences consolidates memories and biases cognition. *Trends Cogn. Sci.* **23**, 876–890 (2019).
46. Schultz, W., Dayan, P. & Montague, P. R. A neural substrate of prediction and reward. *Science*. **275**, 1593–1599 (1997).
47. Bouton, M. E. Context, ambiguity, and unlearning: sources of relapse after behavioral extinction. *Biol. Psychiatry* **52**, 976–986 (2002).
48. Nasser, H. M. & McNally, G. P. Appetitive-aversive interactions in pavlovian fear conditioning.

Behav. Neurosci. **126**, 404–422 (2012).

49. Kandel, E. R., Dudai, Y. & Mayford, M. R. The molecular and systems biology of memory. *Cell* **157**, 163–186 (2014).
50. Izquierdo, I. *et al.* Different molecular cascades in different sites of the brain control memory consolidation. *Trends Neurosci.* **29**, 496–505 (2006).
51. Floresco, S. B. & Tse, M. T. Dopaminergic regulation of inhibitory and excitatory transmission in the basolateral amygdala-prefrontal cortical pathway. *J. Neurosci.* **27**, 2045–2057 (2007).
52. Faul, F., Erdfelder, E., Lang, A.-G. & Buchner, A. G*Power 3: A flexible statistical power analysis program for the social, behavioral, and biomedical sciences. *Behav. Res. Methods* **39**, 175–191 (2007).
53. Cover, K. K., Maeng, L. Y., Lebrón-Milad, K. & Milad, M. R. Mechanisms of estradiol in fear circuitry: Implications for sex differences in psychopathology. *Transl. Psychiatry* **4**, (2014).
54. Stark, R. *et al.* Influence of the stress hormone cortisol on fear conditioning in humans: Evidence for sex differences in the response of the prefrontal cortex. *Neuroimage* **32**, 1290–1298 (2006).
55. Rey, C. D., Lipps, J. & Shansky, R. M. Dopamine D1 receptor activation rescues extinction impairments in low-estrogen female rats and induces cortical layer-specific activation changes in prefrontal-amygdala circuits. *Neuropsychopharmacology* **39**, 1282–1289 (2014).
56. Willenbockel, V. *et al.* Controlling low-level image properties: the SHINE toolbox. *Behav. Res. Methods* **42**, 671–684 (2010).
57. Spielberger, C. D., Gorsuch, R. L. & Lushene, R. E. Manual for the state-trait anxiety inventory. *Consult. Psychol. Press* (1970).
58. Contin, M. & Martinelli, P. Pharmacokinetics of levodopa. *J. Neurol.* **257**, (2010).
59. Hayes, S. C. *et al.* Measuring experiential avoidance: a preliminary test of a working model. *Psychol. Rec.* **54**, 553–578 (2004).
60. Goldberg, D. P. & Hillier, V. F. A scaled version of the General Health Questionnaire. *Psychol. Med.* **9**, 139–145 (1979).
61. Dawson, M. E., Schell, A. M. & Filion, D. L. The electrodermal system. *Handb. Psychophysiology*, *Fourth Ed.* 217–243 (2007) doi:10.1017/9781107415782.010.
62. Feinberg, D. A. *et al.* Multiplexed echo planar imaging for sub-second whole brain fmri and fast diffusion imaging. *PLoS One* **5**, (2010).
63. Staresina, B. P., Alink, A., Kriegeskorte, N. & Henson, R. N. Awake reactivation predicts memory in humans. *Proc. Natl. Acad. Sci.* **110**, 21159–21164 (2013).
64. Shen, X. *et al.* Using connectome-based predictive modeling to predict individual behavior from brain connectivity. *Nat. Protoc.* **12**, 506–518 (2017).

Figure Legends

Fig. 1 Experimental design and skin conductance responses. **a** A three-day fMRI paradigm was employed with fear conditioning on day 1 in context A, extinction on day 2 in context B, and test on day 3 first in context B (the context in which the extinction learning took place), and then in a new context C. Immediately after extinction learning, participants were administered either a placebo or a L-DOPA pill. Drug administration was randomized and double-blinded (placebo: n=35, L-DOPA n=35, all male, for group characteristics, see Supplementary Table 1). All three phases occurred in the MRI scanner. Further, resting-state scans (R) were collected before and after fear learning, before the start of extinction, ~10, 45 and 90 minutes after extinction, and before test. **b** Conditioned responses (CRs) were assessed as SC responses (SCRs) to the CS+ and CS- throughout all experimental phases. The upper panel depicts the mean SCRs of the placebo group (n=33/27/30 on days 1/2/3), the lower panel shows results of the L-DOPA-treated group (n=33/24/25 on days 1/2/3). Data is presented as mean \pm standard error of the mean (sem). **c** Saliva samples were collected on day 2 before the start of the experimental paradigm (time 0 min) followed by a resting-state scan (approx. 8 min) and extinction (approx. 15 min). Subsequent saliva samples were taken right after extinction before pill intake and then about every 20 minutes (+/- 2 minutes), with the last sample taken after the last resting-state measurement at 90 min post-extinction. Samples on day 1 and 3 were collected before and after the paradigm in the scanner (not shown). Tubes represent saliva sample collections. Scanner bore symbols represent scanning times.

Fig. 2 Relationship between CRs at the end of extinction (end-fear) on day 2 and CRs at test in the extinction context B and a new context C on day 3. Extinction success (assessed by differential CRs (CS+>CS-) at the end of extinction) positively predicted spontaneous recovery (differential CRs (CS+>CS-) at test in extinction context B; **(a)** and renewal (differential CRs (CS+>CS-) at test in a new context; **(b)** in both the placebo- and the L-DOPA-treated groups.

Fig. 3 Number of spontaneous reactivations of early CS+ offset-related vmPFC patterns 90 min post-extinction on day 2 predicts CRs at test on day 3 in both groups. Extinction memory retrieval prediction by number of vmPFC reactivations was observed across both L-DOPA- and placebo-treated participants 90 min after extinction. Regression line applies to both groups.

Fig. 4 Effect of post-extinction L-DOPA administration on the number of spontaneous reactivations of CS+ offset-related vmPFC patterns during resting-state scans on day 2. There was no effect of L-DOPA on numbers of vmPFC reactivation patterns during resting-state fMRI 10, 45, and 90 min post extinction learning (n=46). Data is presented as median \pm 1.5*IQR.

Fig. 5 sAA and sCORT measurements on day 2 and relationship between sAA before extinction and CRs at test in context B on day 3. **a** sAA (left panel) and sCORT (right panel) levels exhibited linear decreases on day 2 with peak levels observed before extinction. Saliva samples were collected as presented in Fig. 1c. Data is presented as median \pm 1.5*IQR. Whereas high sAA before extinction was predictive for impaired memory retrieval at test in the extinction context B (spontaneous recovery) in the placebo group (**b**), this effect was rescued by L-DOPA administration (**c**).

Fig. 6 Relationship between sAA before extinction and number of vmPFC reactivations 90 min after extinction learning. **a** High sAA before extinction showed a trend-wise negative association with vmPFC reactivations 90 min after extinction in the placebo-treated group, whereas this effect was abolished in the L-DOPA treated group (**b**).

Figure 7. Pre-extinction LC network functional connectivity is associated with sAA levels before extinction. Circle plot of identified LC network at rest pre extinction, showing all brain regions with at least one highly sAA-predictive edge (significant correlation $>90\%$ of all CPM leave-one-out iterations). Regions with a number of ≥ 5 predictive connections are marked in the plot and displayed on the right. The dACC, vmPFC, and the ventral striatum had the highest number of predictive connections and thus contributed most to the network's predictive power. L/R = left/right, dACC(1)/(2) = dorsal anterior cingulate cortex, dmPFC = dorsomedial prefrontal cortex, vmPFC = ventromedial prefrontal cortex, vStr = ventral striatum.

Supplementary Figure Legends

Supplementary Figure 1. US-expectancy ratings towards CS+ and CS- at all phases. US-expectancy ratings towards the CS+ (left) and the CS- (right) in both groups throughout all experimental phases. Fear acquisition on day 1 was equally successful in both groups based on subjective ratings, as indicated by a significant effect of stimulus (CS+>CS- ratings after fear acquisition: $F_{1,68}=246.56$, $p<.001$, generalized $\eta^2=.65$) in the absence of group (placebo/L-DOPA) and stimulus by group effects ($ps>.18$; $n=70$). Fear was retrieved at the beginning of extinction on day 2 in both groups (stimulus: $F_{1,65}=123.58$, $p<.001$, generalized $\eta^2=.54$; group: $F_{1,65}=0.68$, $p=.41$; stimulus*group: $F_{1,65}=4.38$, $p=.04$, generalized $\eta^2=.04$, interaction based on higher ratings towards the CS+ in the placebo group: two-sample t-test: $t_{65} =2.18$, $p=.03$, CI 95% [-23.91 -1.04], two-sample t-test CS-: $p=.26$; $n=67$) and successfully extinguished on day 2 (stimulus: $F_{1,65}=20.34$, $p<.001$, generalized $\eta^2=.12$; group: $F_{1,65}=0.55$, $p=.46$; stimulus*group: $F_{1,65}=4.37$, $p=.04$, generalized $\eta^2=.03$, two-sample t-tests between groups for CS+ and CS- $ps>.10$; $n=67$). Administration of L-DOPA on day 2 did not result in a significant group difference on day 3 based on ratings before or after test (group and stimulus*group effects: $ps>.06$). Data is presented as median \pm 1.5*inter quartile range (IQR).

Supplementary Figure 2. Spontaneous CS+ offset-related pattern reactivations 90 min post extinction on day 2 in control regions do not predict CR (SCR CS+>CS-) at test on day 3. The number of CS+ offset-related pattern reactivations did not predict CR at test (spontaneous recovery in context B) (multiple linear regression: vmPFC: $\beta=-.07$, $p=.036$; all other $p>.11$; $n=46$).

Supplementary Figure 3. sAA and sCORT measurements on days 1 and 3. sAA (left) and sCORT (right) did not differ on day 1 between groups and time, that is before and after conditioning (sAA: time: $F_{1,59}=2.28$, $p=.14$, group: $F_{1,59}=.72$, $p=.40$, time*group: $F_{1,59}=.88$, $p=.35$, $n=61$, sCORT: time: $F_{1,64}=2.95$, $p=.09$, group: $F_{1,64}=2.78$, $p=.10$, time*group: $F_{1,64}=.28$, $p=.60$, $n=66$). On day 3, only sCORT was significantly decreased after the experimental procedure in both groups (sAA: time: $F_{1,54}=.26$, $p=.62$, group: $F_{1,54}=.29$, $p=.60$, time*group: $F_{1,54}=2.97$, $p=.09$, $n=57$, sCORT: time: $F_{1,57}=10.67$, $p=.002$, group: $F_{1,57}=.07$, $p=.80$, time*group: $F_{1,57}=.18$, $p=.67$, $n=60$). Saliva samples were collected before and after the experimental procedure on day 1 and 3. Data is presented as median \pm 1.5*IQR.

Supplementary Figure 4. Relationship between pre-extinction sAA and end-fear of extinction, and between pre-extinction sCORT and CRs at test. **a** An exploratory analysis revealed that peak sAA levels were associated at trend level with high extinction end-fear, that is, poor extinction success ($p=.08$). **b** Peak sCORT predicted CRs at spontaneous recovery, however, in the opposite direction (more sCORT – less spontaneous recovery; ($p=.02$)).

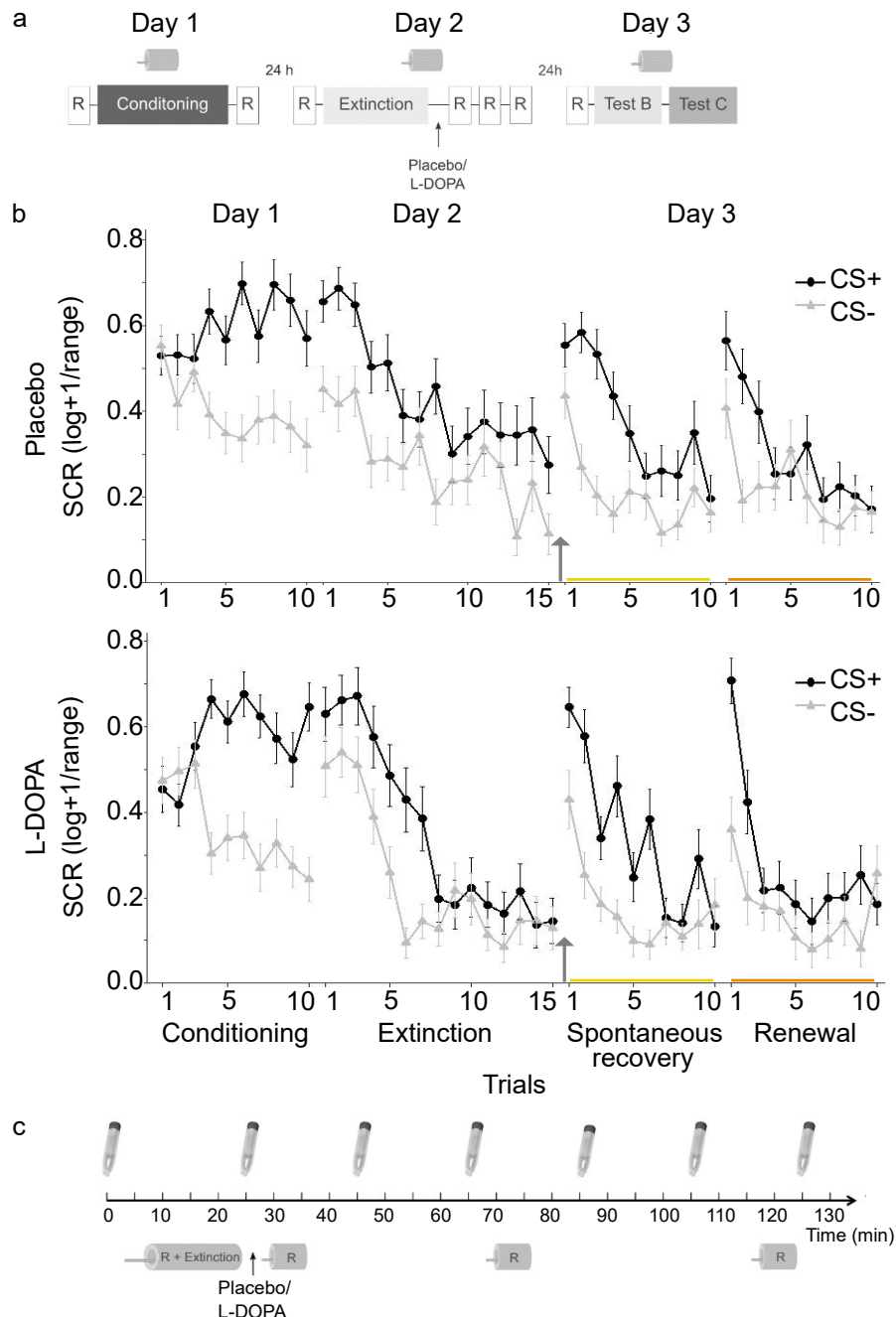


Figure 1

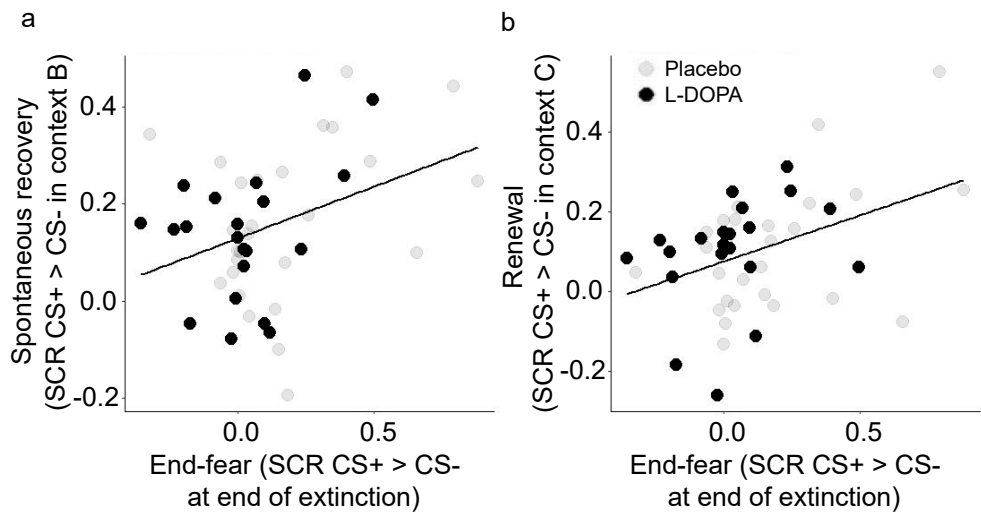


Figure 2

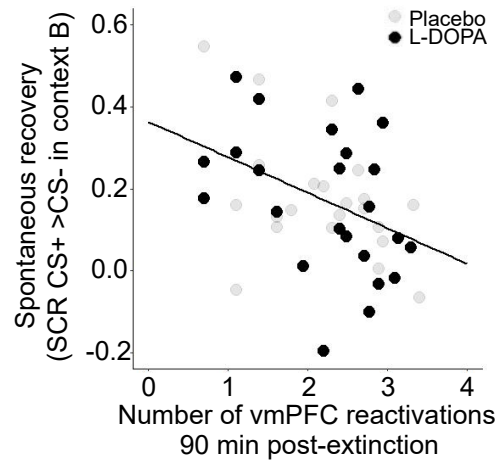


Figure 3

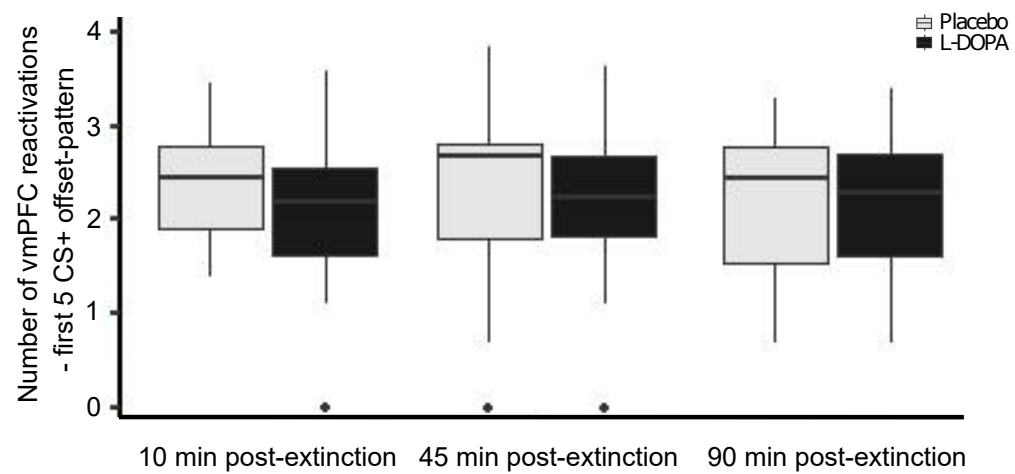


Figure 4

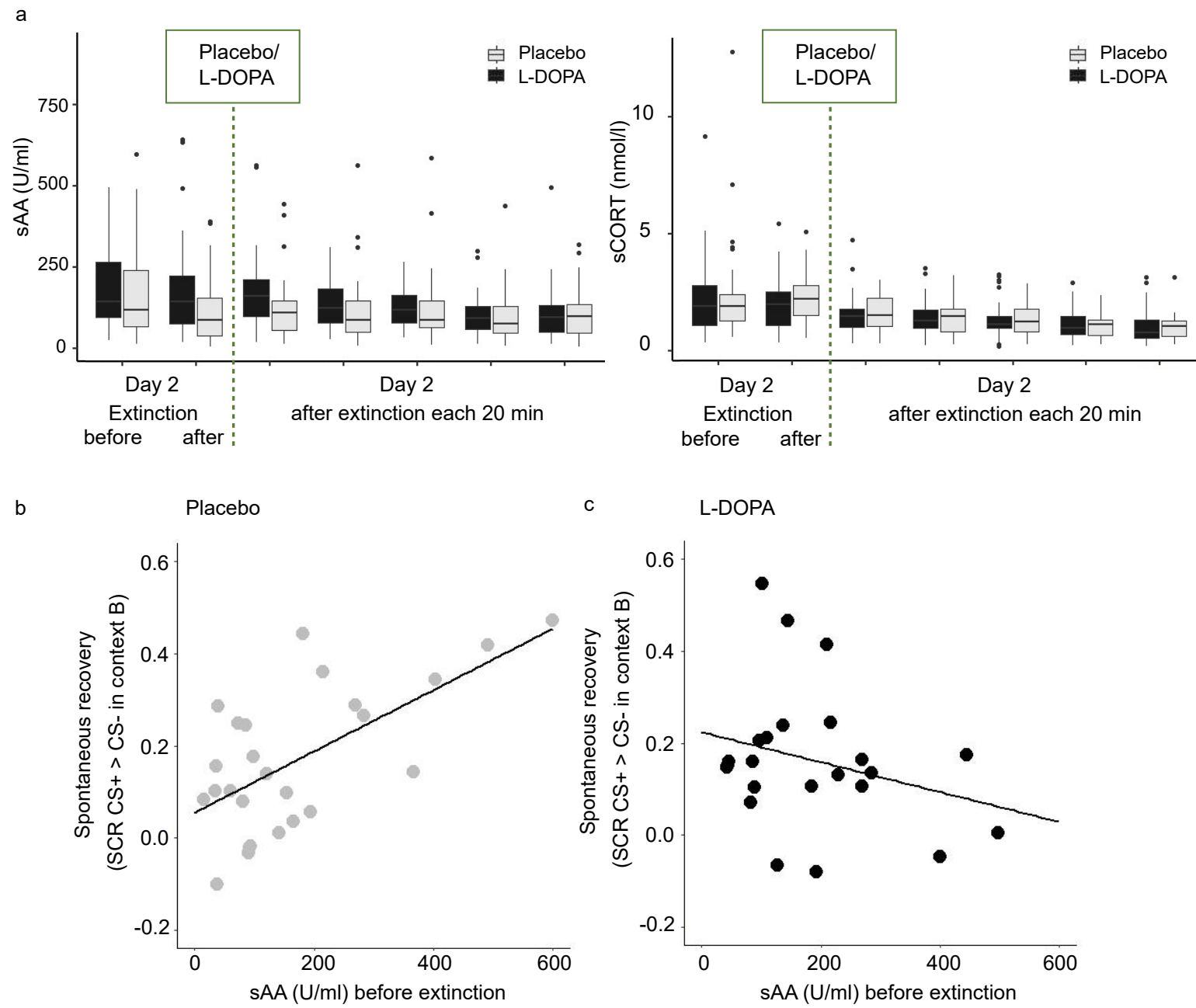


Figure 5

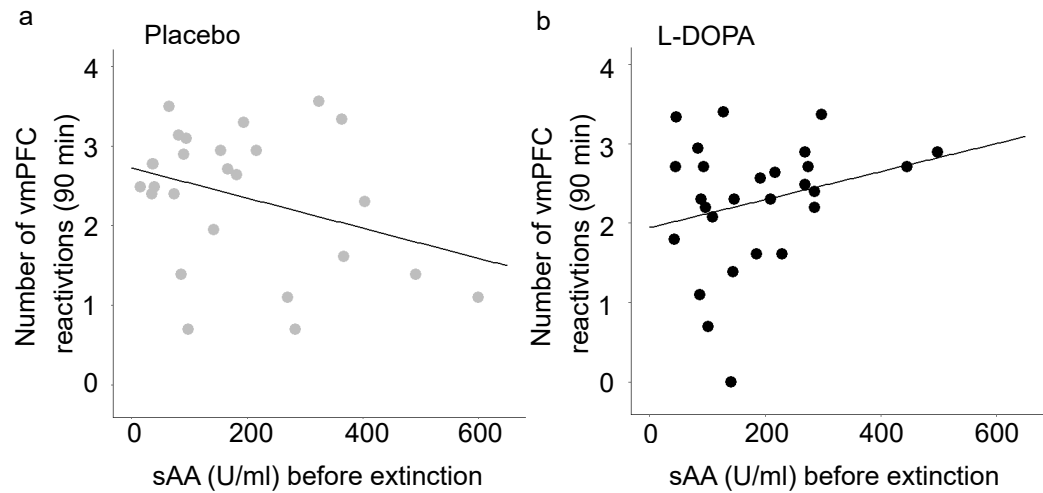


Figure 6

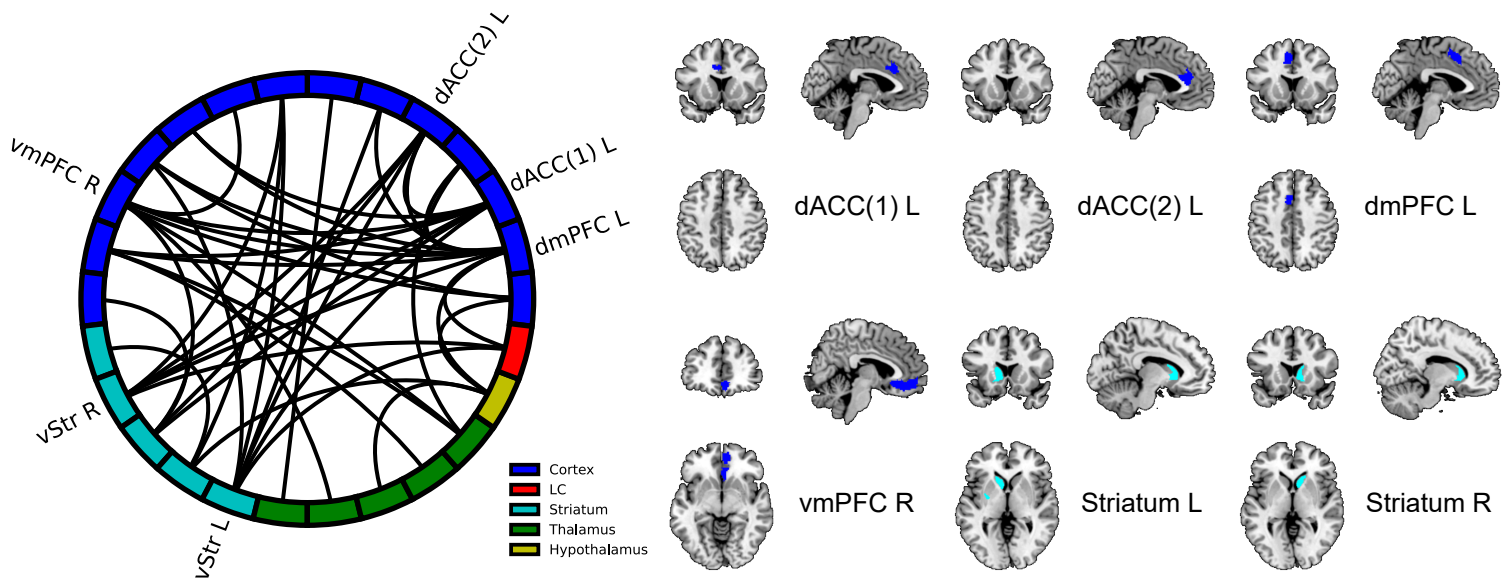
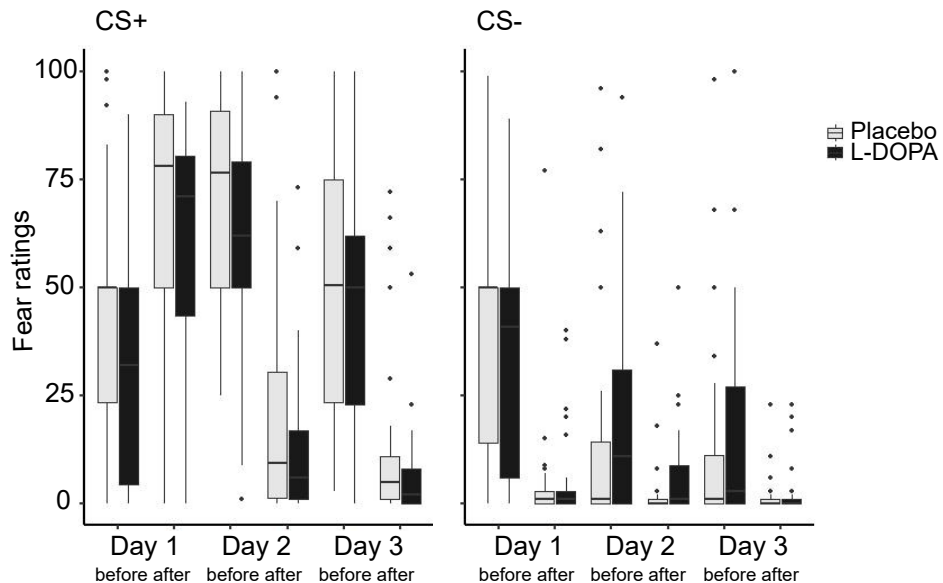
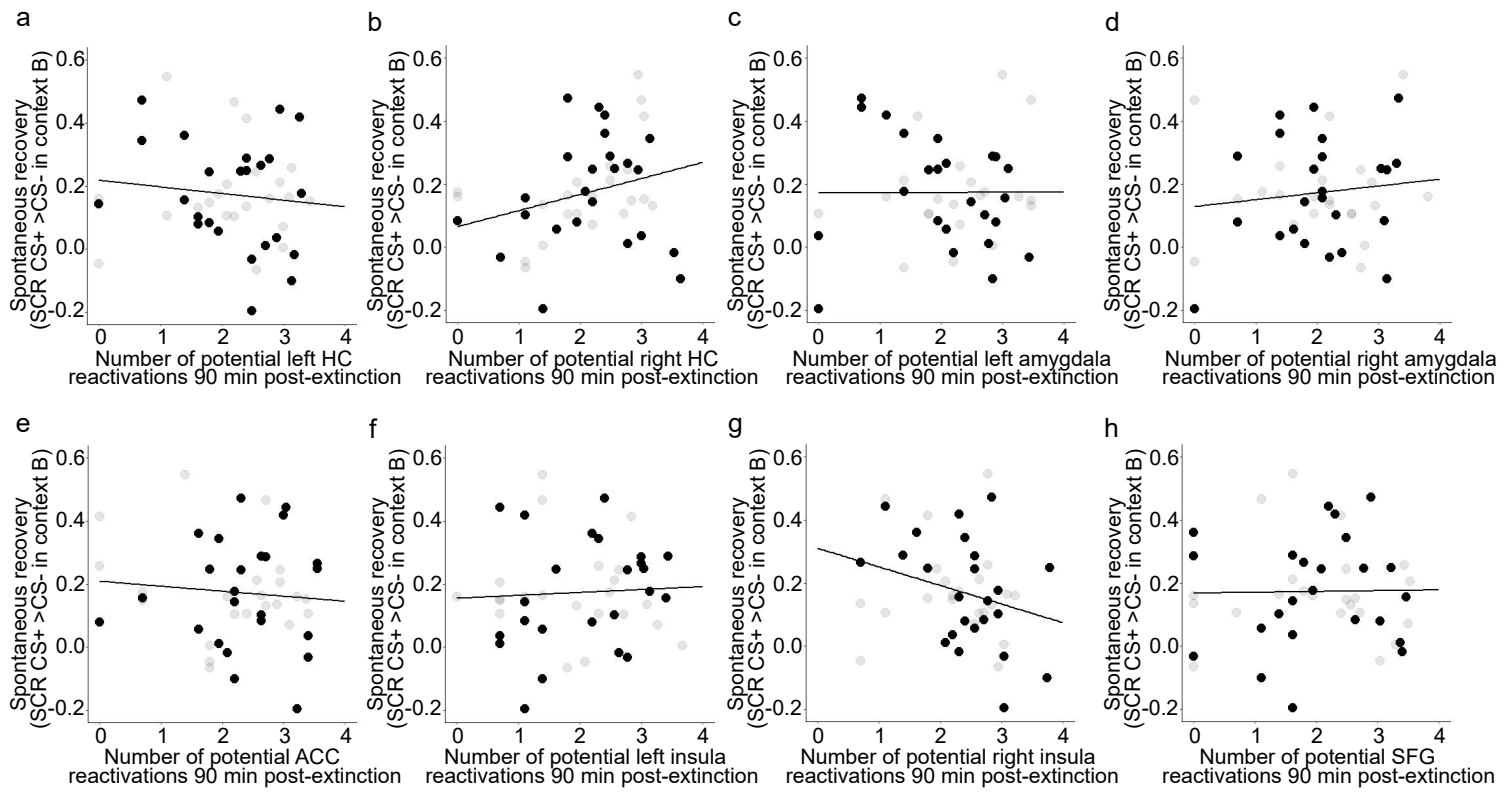


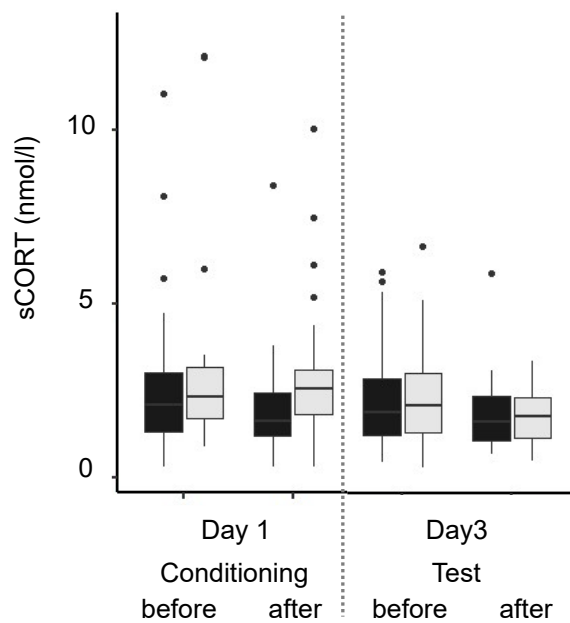
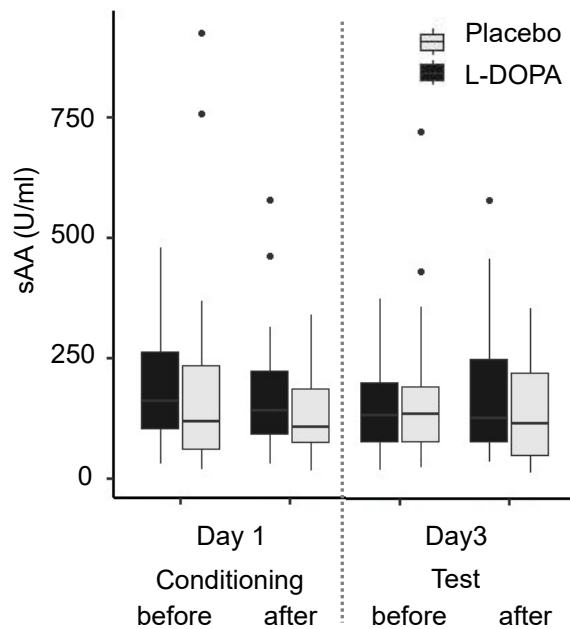
Figure 7



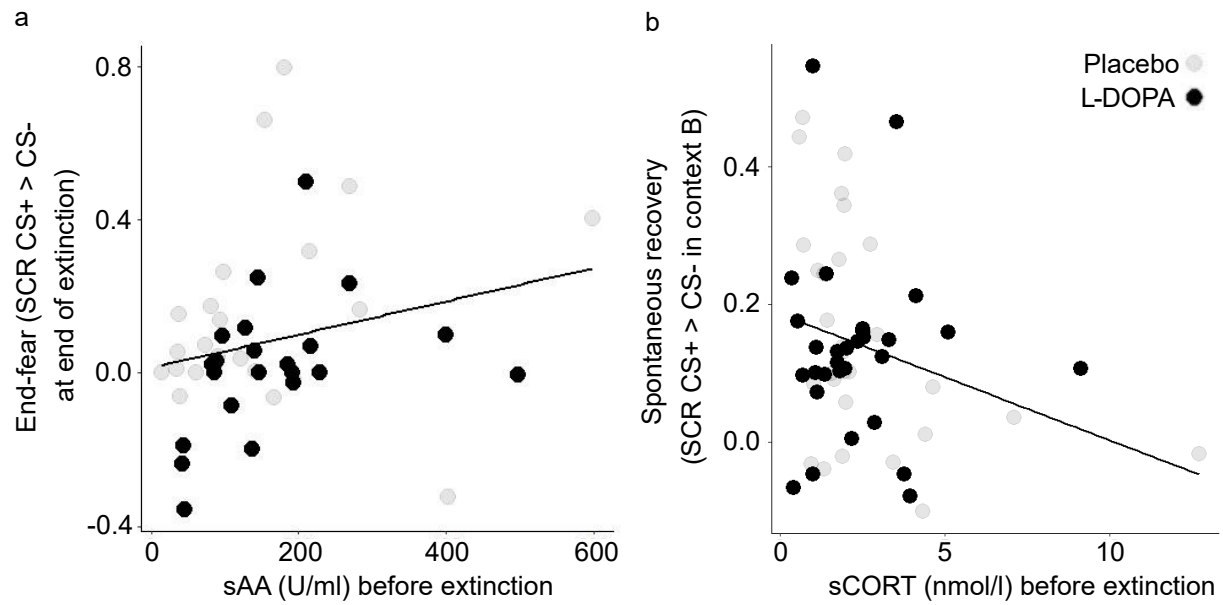
Supplementary Figure 1



Supplementary Figure 2



Supplementary Figure 3



Supplementary Figure 4